electronics

MDPI

Article

An Experiment-Based Comparison between Fully Digital and Hybrid Beamforming Radio Architectures for Many-Antenna Full-Duplex Wireless Communication

Gavin Megson [1], Sabyasachi Gupta [2], Syed Muhammad Hashir [2], Ehsan Aryafar [1,*] and Joseph Camp [2]

[1] Department of Computer Science, Portland State University, Portland, OR 97201, USA; gmegson@pdx.edu
[2] Lyle School of Engineering, Southern Methodist University, Dallas, TX 75275, USA; sabyasachig@smu.edu (S.G.); hashirs@smu.edu (S.M.H.); camp@smu.edu (J.C.)
* Correspondence: earyafar@pdx.edu

Abstract: Full-duplex (FD) communication in many-antenna base stations (BSs) is hampered by self-interference (SI). This is because a FD node's transmitting signal generates significant interference to its own receiver. Recent works have shown that it is possible to reduce/eliminate this SI in fully digital many-antenna systems, e.g., through transmit beamforming by using some spatial degrees of freedom to reduce SI instead of increasing the beamforming gain. On a parallel front, hybrid beamforming has recently emerged as a radio architecture that uses multiple antennas per FR chain. This can significantly reduce the cost of the end device (e.g., BS) but may also reduce the capacity or SI reduction gains of a fully digital radio system. This is because a fully digital radio architecture can change both the amplitude and phase of the wireless signal and send different data streams from each antenna element. Our goal in this paper is to quantify the performance gap between these two radio architectures in terms of SI cancellation and system capacity, particularly in multi-user MIMO setups. To do so, we experimentally compare the performance of a state-of-the-art fully digital many antenna FD solution to a hybrid beamforming architecture and compare the corresponding performance metrics leveraging a fully programmable many-antenna testbed and collecting over-the-air wireless channel data. We show that SI cancellation through beam design on a hybrid beamforming radio architecture can achieve capacity within 16% of that of a fully digital architecture. The performance gap further shrinks with a higher number of quantization bits in the hybrid beamforming system.

Keywords: Full-Duplex; MU-MIMO; self-interference; interference cancellation

Citation: Megson, G.; Gupta, S.; Hashir, S.M.; Aryafar, E.; Camp, J. An Experiment-Based Comparison between Fully Digital and Hybrid Beamforming Radio Architectures for Many-Antenna Full-Duplex Wireless Communication. *Electronics* **2022**, *11*, 59. https://doi.org/10.3390/electronics11010059

Academic Editor: Pal Varga

Received: 10 December 2021
Accepted: 23 December 2021
Published: 25 December 2021

1. Introduction

When a wireless communication device attempts to send a stream of data while receiving a different stream, two common techniques are time-division duplex, where intervals alternate to allow each stream a portion of time to send some of its data, and frequency-division duplex, where the allocated frequency band is split between streams. The majority of existing systems operate in one of these two modes. Since the data rate scales with both time and frequency, the maximum rate for each stream in both of these scenarios is theoretically half of what it would be if each stream could use the entire frequency band for the entire time period. This latter approach is known as full-duplex (FD) communication.

The main barrier to FD communication is self-interference (SI). Because the transmitter of a device would be very close to its receiver, it can drown out the stream the device is attempting to receive, potentially causing frequent outages [1,2]. When a FD device has a small number of antennas, clever antenna placement can cancel out SI [3–7]. However, in modern many-antenna base stations (BSs), such as cellular towers, which use multiple antennas to send and receive with greater directionality (known as multiple-input and multiple-output systems, or MIMO), this method does not work. There is a growing body of research dedicated to the fundamental trade-off between beamforming gain and SI in

many-antenna BSs, and to developing algorithms to maximize gain while minimizing interference [3–10].

When developing techniques to reduce SI, assumptions must be made about the underlying hardware involved. There are two main architecture types for many-antenna BSs (Figure 1). In fully digital architectures, each transmitting antenna is connected to its own RF chain, which can fine tune the phase and amplitude of the signal transmitted from that antenna. In hybrid architectures, some antennas share RF chains, often via an FPGA, resulting in less control over the amplitude but usually preserving control over the phase of a signal.

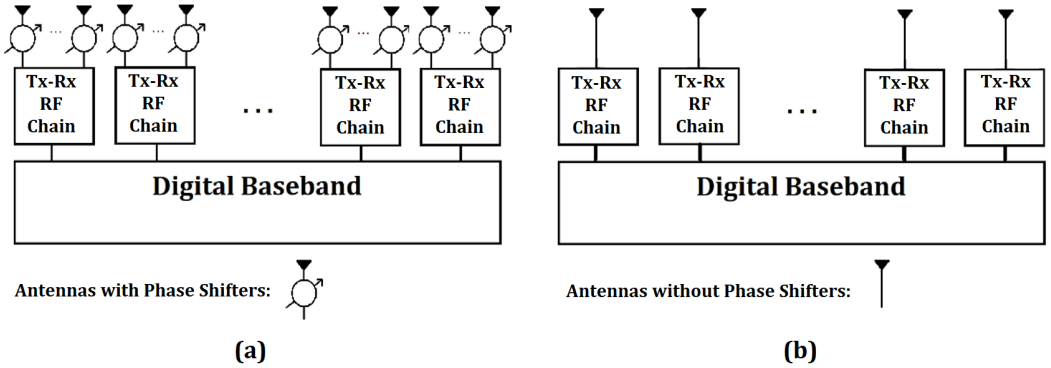

Figure 1. (**a**) Example hybrid architecture. Each RF chain sends the same signal to multiple connected antennas, altered only by phase shifters. (**b**) Example fully digital architecture. Every antenna has its own RF chain attached, allowing for more complete signal control but increasing hardware costs.

For both architectures, existing solutions with decent performance in certain scenarios exist [11–13], but not every technique was designed to scale into many-antenna BSs and/or multi-user MIMO (MU-MIMO) scenarios, where a many-antenna BS may communicate with different clients at the same time and frequency.

In this work, we investigate the performance trade-offs between hybrid and digital architectures for FD many-antenna base stations. Using real-world channel measurements from our custom 32-antenna BS and multiple-client setup, we compare the performance of full-duplex BSs with hybrid and fully digital architectures in single-user and multiple-user MIMO scenarios as the number of clients increases. Our key contributions are as follows:

- Implementation. We implemented two SI cancellation techniques on a fully programmable 32-antenna FPGA testbed: (i) a state-of-the-art technique (SoftNull [13]), which is designed for fully digital architectures, and (ii) M-HBFD (Multi-User Hybrid FD), which is an adaptation of SoftNull that we developed to reduce SI in hybrid beamforming architectures.
- Channel Measurement. We gathered thousands of real-world channel measurements in an indoor multi-path rich environment to experimentally compare the performance of the two systems.
- SI and Sum Capacity Rate. We show that with five bits of phase quantization, M-HBFD achieves close to 90% of SoftNull capacity with 15–25% increase in SI.
- Capacity per RF Chain. We evaluated the relative capacity for each technique normalized by the number of RF chains utilized by the BS architecture for each technique. We show that M-HBFD can provide up to 15x increase in per RF chain capacity when all antennas are used to communicate with only a single client.

The rest of this paper is organized as follows. In Section 2, we discuss the background information and related work. In Section 3, we formalize the system definition. In Section 4, we discuss the SI cancellation techniques for both radio architectures. In Section 5, we describe our experimental setup for channel measurements. In Section 6, we describe our evaluation methodology. In Section 7, we present and discuss our findings. We conclude in Section 8.

2. Background and Related Work

2.1. Background

2.1.1. Architecture

There are two main architecture types for many-antenna base stations. In hybrid architectures, one RF chain is connected to multiple antennas, resulting in less control over the amplitude of the signal at each antenna but retaining some control over the phase through a phase shifter. A phase shifter on each antenna element shifts the phase of the signal by a complex coefficient with constant amplitude. In practice, a phase shifter is a discrete quantized component with a few bits of resolution. For example, the phase of a 2-bit phase shifter is selected from the set $\{0^\circ, 90^\circ, 180^\circ, 270^\circ\}$.

Some hybrid architectures connect every RF chain to every antenna in parallel (an arrangement known as a fully connected hybrid architecture), although this can be difficult to implement at scale [14]. More often, antennas are connected to only one RF chain in an array, creating independent subarrays. A typical hybrid architecture is depicted in Figure 1a.

In fully digital architectures, each transmitting antenna is connected to its own RF chain, as in Figure 1b. Since each antenna can send a signal formed completely independently of the others, fully digital hardware has greater freedom for beamforming and, thus, tends to outperform hybrid architectures. However, the increased number of full RF chains requires more expensive hardware.

2.1.2. Massive (Many-Antenna) MIMO

The trend in wireless BSs is toward using an ever increasing amount of antennas, and communicating with an increasing number of clients simultaneously (known as massive multi-user MIMO, or massive MU-MIMO) [15–18]. With more antennas comes greater directionality in beamforming, leading to better signal quality and, thus, greater data rates and more efficient use of resources. Since each client typically requires its own independent stream of data, the maximum number of clients a BS can send a signal to simultaneously is bounded by the number of RF chains a BS has. However, it is not always efficient to communicate with this number of clients, and, in many-antenna systems, the ratio between the number of antennas at the BS and the total number of antennas across all clients is high.

2.2. Related Work

2.2.1. Hybrid Architecture Full-Duplex

Hybrid architectures can sometimes yield sizable reductions in SI without increasing the number of RF chains [11,12,19–21]. In Phased Array Full-Duplex [11], the optimal trade-off between beamforming gain and SI when only adjusting the phase of the antenna elements is estimated with a semidefinite relaxation. When the SI at each of the receive antennas is highly correlated, such as in linear arrays, PAFD performs well. For planar arrays, researchers have created an algorithm [12] which jointly forms a transmit and a receive beam in an iterative method that converges on the optimal solution. Although an iterative process that requires all beams to form together will face challenges scaling up to multi-user BS scenarios, when communicating with two clients in FD the algorithm performs well. Several other attempts at SI cancellation have included alterations to the underlying hardware outside the scope of this paper [19,22–24].

2.2.2. Digital Architecture Full-Duplex

Due to their greater flexibility in output, fully digital architectures tend to outperform hybrid architectures for complex many-antenna BSs attempting FD communication [13,25,26]. For example, SoftNull [13] is a leading fully digital algorithm which reduces SI while explicitly preserving a desired number of antennas for beamforming use. One way to do this would be to simply take the antennas which contribute most to SI and set their output to zero. SoftNull takes a similar approach, but increases the efficacy by first taking a singular value decomposition of the SI matrix between all transmit and receive

antennas and setting the highest correlated vectors to zero instead. For example, if a higher level application wanted to beamform with 6 antennas on a 9-antenna transmit array, SoftNull nulls the 3 linear combinations of transmit antennas which contribute most to SI and takes the remaining 6 as the usable, "effective" antennas to use for beamforming as the application chooses.

2.2.3. Trade-Off between Architectures

Although a typical hybrid architecture exhibits no independent control over the amplitude of a signal at each antenna, some methods have been implemented [14,27,28] and shown to improve beamforming gain over phase-only manipulation. However, previous research has not focused on FD communication, and typically assumed communicating with a small number of clients, posing difficulty for adaptation to MU-MIMO BSs.

In previous research [29], we assumed an architecture which is not fully digital but allows discrete levels of amplitude in addition to phase control. We showed that in one-downlink, one-uplink scenarios, a close enough discrete approximation to a fully digital algorithm results in similar performance while using far fewer RF chains.

3. System Definition

A base station has M antennas arranged rectangularly, divided into a transmit array with M_{Tx} antennas and a receive array of M_{Rx} antennas, where $M_{Tx} + M_{Rx} \leq M$. The BS communicates with K_{up} half-duplex uplink clients and K_{down} half-duplex downlink clients simultaneously. Each uplink/downlink client is equipped with only a single antenna.

A transmit array of M_{Tx} antennas is comprised of R_{Tx} rows of C_{Tx} antennas, where $R_{Tx} \times C_{Tx} = M_{Tx}$. Similarly, a receive array of M_{Rx} antennas is comprised of R_{Rx} rows of C_{Rx} antennas, where $R_{Rx} \times C_{Rx} = M_{Rx}$. For ease of discussion, in this paper, "rows" run side to side, perpendicular to the division between transmit and receive arrays, and "columns" run parallel to the division. A row in a transmit array will have one end close to the receive array and one end far away (see Figure 2).

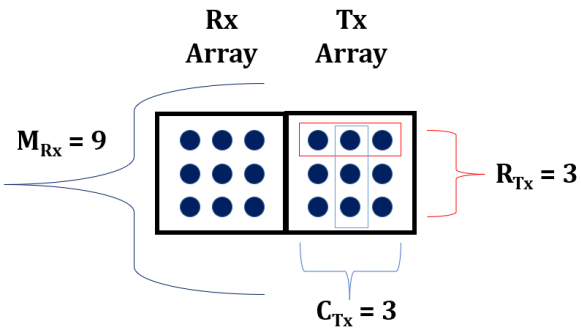

Figure 2. Example base station with $M_{Rx} = M_{Tx} = 9$ and $R_{Tx} = C_{Tx} = R_{Rx} = C_{Rx} = 3$.

A transmit array consists of N_{Tx} subarrays, where N_{Tx} can be any whole factor of R_{Tx} where $1 \leq N_{Tx} \leq R_{Tx}$. A transmit subarray is a subset of the transmit array consisting of R_{Tx}/N_{Tx} contiguous rows. Similarly, a receive array consists of N_{Rx} subarrays, where N_{Rx} can be any whole factor of R_{Rx}, where $1 \leq N_{Rx} \leq R_{Rx}$. A receive subarray is a subset of the receive array consisting of R_{Rx}/N_{Rx} contiguous rows. Concatenating these subarrays will reproduce the original array.

The self-interference channel matrix between the transmit and receive arrays is denoted H_{self}, where $H_{self} \in \mathbb{C}^{M_{Tx} \times M_{Rx}}$. The uplink channel matrix is $H_{up} \in \mathbb{C}^{M_{Rx} \times K_{up}}$, and the downlink channel matrix is $H_{down} \in \mathbb{C}^{M_{Tx} \times K_{down}}$.

The SI channel matrix between a transmit subarray and the receive array is $H_{sub_{i,all}} \in \mathbb{C}^{M_{Tx}/N_{Tx} \times M_{Rx}}$. Similarly, the SI channel matrix between a receive subarray and the transmit array is $H_{sub_{all,j}} \in \mathbb{C}^{M_{Rx}/N_{Rx} \times M_{Tx}}$. The SI channel matrix between any two transmit and receive subarrays is denoted $H_{sub_{i,j}} \in \mathbb{C}^{M_{Tx}/N_{Tx} \times M_{Rx}/N_{Rx}}$.

The channel matrix between the uplink clients and the receive array is $H_{up} \in \mathbb{C}^{K_{up} \times M_{Rx}}$. The channel matrix between the uplink clients and a receive subarray is $H_{up_j} \in \mathbb{C}^{K_{up} \times M_{Rx}/N_{Rx}}$. The channel matrix between the transmit array and the downlink clients is $H_{down} \in \mathbb{C}^{K_{down} \times M_{Tx}}$. The channel matrix between a transmit subarray and the downlink clients is $H_{down_i} \in \mathbb{C}^{K_{down} \times M_{Tx}/N_{Tx}}$.

The vector of symbols transmitted by the transmit array is $x_{down} \in \mathbb{C}^{M_{Tx}}$. The vector of symbols transmitted by the uplink clients is $x_{up} \in \mathbb{C}^{K_{up}}$.

The signal received at the receive array is:

$$y_{up} = H_{up}x_{up} + H_{self}x_{down} + z_{up}, \quad (1)$$

where $z_{up} \in \mathbb{C}^{M_{Rx}}$ is noise.

The signal received at the downlink clients is:

$$y_{down} = H_{down}x_{down} + z_{down}, \quad (2)$$

where $z_{down} \in \mathbb{C}^{K_{down}}$ is noise. For ease of discussion, this model assumes negligible client to client interference.

4. Algorithmic Implementation

4.1. Architectural Assumptions

The BS assumed in this paper requires hardware similar to a typical hybrid architecture, but with the ability to control amplitude discretely between specific levels. In particular, we have specified the number of those levels at various powers of 2, and their power levels at equal divisions between zero and a maximum. Similar archetectures matching this description exist [14,27,28], but with far fewer RF chains, and sometimes with different connection choices between RF chains and antennas.

4.2. Algorithm Design

To compare digital and hybrid MU-MIMO performance, we choose SoftNull [13] as the representative of leading fully digital techniques. In this section, we first describe the key components of SoftNull and our proposed adaptation of SoftNull when applied to a hybrid beamforming radio architecture. We refer to our proposed approach as Multi-User Hybrid FD and denote it as M-HBFD.

4.2.1. Key Components of SoftNull

SoftNull is divided into two main stages: a standard MU-MIMO precoder (denoted $P_{down} \in \mathbb{C}^{D_{Tx} \times K_{down}}$) which precodes signals between D_{Tx} effective antennas and K_{down} clients, and the SoftNull precoder (denoted $P_{self} \in \mathbb{C}^{M_{Tx} \times D_{Tx}}$) which reduces SI by emulating the beamforming ability of D_{Tx} effective antennas with M_{Tx} physical antennas. Let $s_{down} \in \mathbb{C}^{K_{down}}$ be the vector of symbols the BS sends to each of the K_{down} downlink users. Then, the transmitted vector of symbols is $x_{down} = P_{self}P_{down}s_{down}$.

The standard precoder P_{down} requires no knowledge of the SoftNull precoder and can be any standard precoder, such as zero-forcing. The SoftNull precoder P_{self} reduces BS SI while preserving D_{Tx} effective antennas by taking a singular value decomposition of the SI matrix between all transmit and receive antennas (H_{self}) and setting the ($M_{Tx} - D_{Tx}$) highest correlated vectors to zero. This reduces the dimensionality of the transmit array to D_{Tx} while reducing SI.

Although SoftNull was created from the perspective of trading transmit beamforming for SI reduction, it is equally valid to apply the algorithm to a receive array for the purposes of trading receive beamforming for SI reduction. Then, D_{Tx} becomes D_{Rx}, downlink clients become uplink clients, etc.

4.2.2. M-HBFD Design

We propose to create a viable algorithm for SI cancellation with an MU-MIMO hybrid radio architecture at the BS in the following manner. First, we divide the BS antennas into separate transmit and receive arrays of M_{Tx} and M_{Rx} antennas respectively, as in SoftNull and described in our system definition. Without lack of generality, we describe implementing the algorithm on the transmit array, but the algorithm could similarly be applied to a receive array. We sort all R_{Tx} rows in the transmit array into N_{Tx} subarrays, and each subarray uses a single RF chain to communicate with a single downlink client. For example, if a 4×4 transmit array ($M_{Tx} = 16$, $R_{Tx} = 4$, $C_{Tx} = 4$) needed to communicate with two downlink clients, there would be two 2×4 subarrays ($N_{Tx} = 2$) each communicating with one client, and two total RF chains used for downlink transmission.

For each subarray, SoftNull is calculated specifically for that subarray. The SI matrix used in these calculations, $H_{sub_{i,all}}$, is that between the subarray i and the receive array. The total number of effective antennas for the transmit array are calculated as in SoftNull and then divided equally among subarrays to get the number of effective antennas used for each subarray SoftNull calculation. To extend the earlier example, in the case of $M_{Tx} = 16$ and $N_{Tx} = 2$, if $D_{Tx} = 4$, then each subarray i uses 2 effective antennas to calculate SoftNull, and the singular value decomposition is taken from $H_{sub_{i,all}}$.

For each physical antenna, the corresponding entry in x_{down} is approximated to the closest value achievable, dependent on the number of quantization bits in the architecture. By organizing whole rows into subarrays, we ensure each transmit subarray has antennas similar distances from the receive array. This arrangement helps ensure there is approximately equal SI reduction power between subarrays. With this arrangement, we imply equal importance of communication with each client.

An alternative approach to the one outlined above would be to simply take a discrete approximation of SoftNull as applied on the whole transmit array for any number of clients, without first subdividing the arrays. This approach is likely to produce higher capacity, but is less flexible than subdividing the arrays. For example, whenever there is a change in the location of a single downlink client, the entire transmit array's beam must be recalculated. Even on massive many-antenna arrays, this approach is likely to perform worse with a high number of clients. It also raises questions of computational complexity and requires a fully connected hybrid architecture.

When comparing the performance of M-HBFD against SoftNull, we do not first subdivide the transmit or receive arrays before applying SoftNull. Despite our belief that this will not scale well with the number of clients, we use it as a pessimistic standard when evaluating the MU-MIMO potential of M-HBFD.

5. Data Collection

To perform our analysis, we collected real-world channel measurements with up to 32 antennas at the BS and 4 single-antenna clients.

The channel measurements, for BS self-interference, as well as BS/client communication, were collected using a chain of Skylark Wireless Iris radios with 2.4 GHz frontends (Figure 3a), each Iris radio has two RF chains. The unique feature of these modular radios is their ability to synchronize the clocks across all antennas, thus allowing relative time from transmission to reception to be measured.

Each RF chain is attached to a dipole antenna (Figure 3b). These antennas represent one of two things: a BS array arranged in a 4×8 rectangular pattern spaced at one-half wavelength, or located one meter away in one of five zones equally splitting a 180 degree arc to represent client devices, elevated at 30 degrees (see Figure 4). Dipole antennas in a rectangular array as oriented in this setup may not represent the most useful radiation pattern for a BS; however, client antennas are elevated to stay within the radiation pattern of each BS antenna and avoid occlusion.

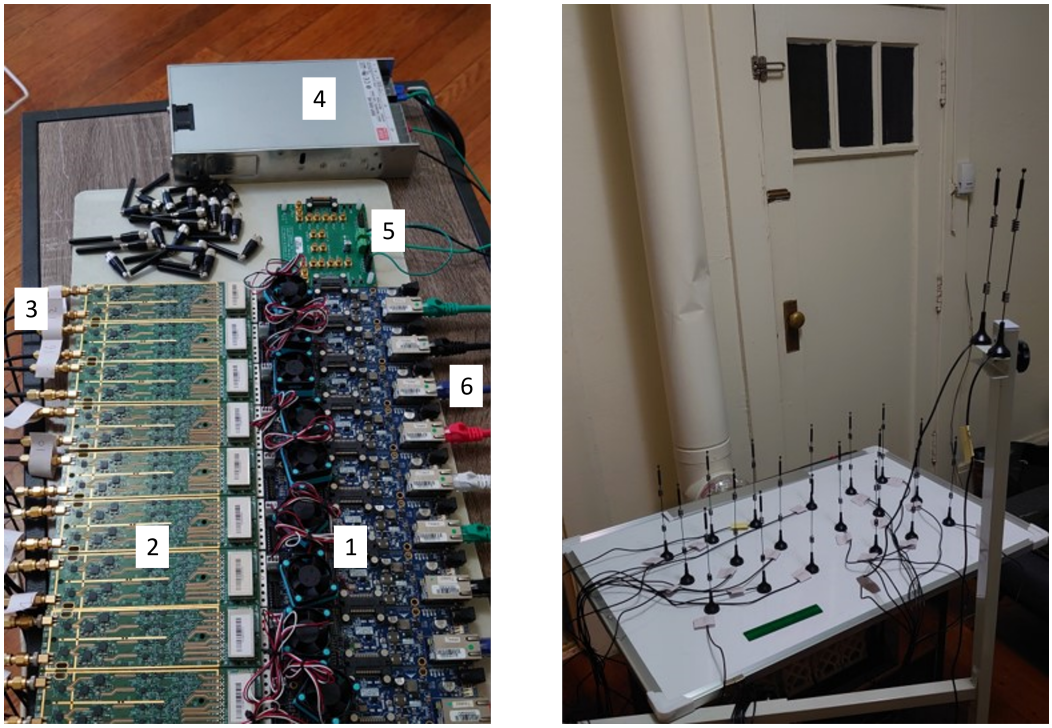

(a) **(b)**

Figure 3. (**a**) Our radio hardware, including Skylark Wireless Iris radios (1) and associated RF front ends (2), antenna cable extensions (3), AC/DC power converter (4) and bus power converter (5), and ethernet connections (6). (**b**) An example antenna layout. In this picture, the antennas are not yet set in their exact test configuration.

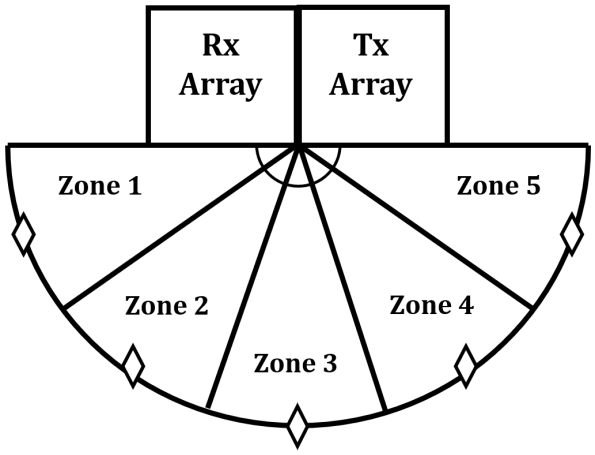

Figure 4. Top-down representation of BS and client zones. Not drawn to scale. Diamonds indicate approximate location of client antennas.

Channel measurements are taken by sending an LTS pilot sequence at 2.484 GHz (WiFi channel 14) from each RF chain one at a time, while every other RF chain listens and stores the raw IQ values in their buffers. The timing information from the synchronized clocks is combined with the received power information from each RF chain to estimate the effective instantaneous channel state information for each pair of antennas. The radios are set up in an indoor high-scattering environment. For each trial, we took the median of 30 observations, spaced over about one minute, as one channel measurement. This method removed outliers while avoiding drifting channel measurements associated with our hardware heating up over time. Custom control code was written in Python and

originally stemmed from existing open-source code [30]. This process was repeated to produce fifteen series of channel measurements between all BS and client antennas.

6. Data Analysis

To compare the results of M-HBFD in different scenarios, we vary the BS array size, the number of effective antennas used in SoftNull, and the number and location of clients the BS communicates with simultaneously.

We compare M-HBFD against SoftNull on the metrics of total SI at the BS, total capacity of all communication streams, and total capacity per RF chain used.

When varying array size, the same collected data is used for each trial. The full BS array is comprised of a 4×4 transmit and a 4×4 receive array. To emulate a smaller BS, the rearmost and sides of the 32-antenna full BS array are simply ignored, to leave an 18-antenna array (comprised of a 3×3 transmit and a 3×3 receive array) in the middle towards the client antennas.

One of the variable inputs to SoftNull is the number of effective antennas, which is directly correlated to beamforming gain. In our experiments, when varying the number of effective antennas, we keep the total number of effective antennas the same for the transmit or receive array as a whole for better comparison of algorithms. For M-HBFD, effective antennas are evenly divided among subarrays. For ease of discussion, in this paper, we characterize the effective antennas in both algorithms as "effective antennas per row". Due to the possible values for array size, in our experiments, the effective antennas per row vary only between 1 and 2.

When varying the number of subarrays, or equivalently, number of clients in simultaneous communication, values are chosen intelligently to produce a constant whole number of rows in each subarray given the sizes of our BS arrays.

When measuring SI, the recorded values are normalized by dividing by the norm (2-norm) of the transmission weight vector to better compare across array variation. SI is calculated based on the total sum received power above the noise floor at all receive antennas, where only the transmission array is implementing SoftNull or M-HBFD, and the receive array is not.

When measuring capacity, both the transmit and receive arrays implement SoftNull or M-HBFD. The number of uplink clients matches the number of downlink clients, and the related subdivision of the receive array matches the subdivision of the transmit array. Since SI is now affected by both arrays, the effective SI can be different from the SI calculated as described above, even when using the same measured SI values.

When calculating capacity per RF chain, the same measured capacity values are used and then divided by the number of RF chains implied with each algorithm. In the case of SoftNull, this number is the number of antennas in the entire array, either 32 or 18. In the case of M-HBFD, this number is the number of subarrays (on both the transmit and receive array combined), or equivalently, the number of clients in communication (both uplink and downlink).

In both SI and capacity calculations, specific clients need to be chosen. For both uplink and downlink, random clients are chosen, without repeating a choice, between all 15 trials. Since there are only two uplink and two downlink client antennas per zone in each trial, a maximum of two clients from the same zone can be selected to communicate with either the transmit or receive array in any trial. In the case of capacity measurement, where both uplink and downlink clients are chosen, uplink and downlink clients are chosen independently, whereas, in the case of SI measurement only, downlink clients are chosen.

We also compare the SI generated when transmitting to clients in different zones. In this comparison, we vary array size and effective antennas but only communicate with one client at a time, using the whole transmit array. One of the two downlink client antennas in each zone was chosen at random for each trial.

7. Results and Analysis

7.1. Quantization

We first investigate the effect of the number of quantization bits on M-HBFD's performance. Figure 5 shows the change in total capacity as the value at each antenna is allowed more and more possible values. For each number of quantization bits from 1–8 depicted, each data point is the geometric mean of 15 trials broken down by array size, number of subarrays, and number of effective antennas per row, for a total of 10 data points per level.

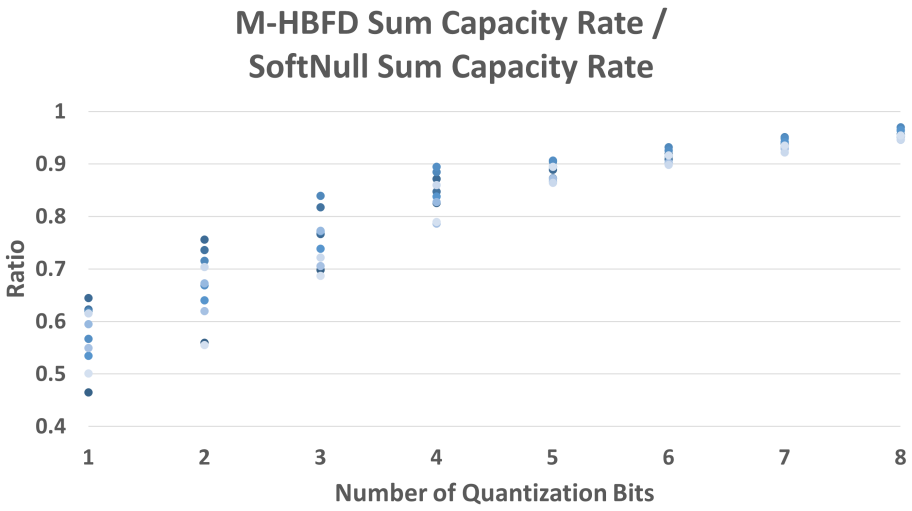

Figure 5. Effect of the number of quantization bits on the ratio of M-HBFD sum capacity rate to SoftNull.

Although the number of quantization bits acceptable to use in each use case depends on both hardware considerations, as well as accuracy requirements, to proceed with further performance comparisons, we select 5 bits as the baseline level of quantization for M-HBFD.

7.2. Client Zones

The effect of the zone of a downlink client to its effect on SI compared to SoftNull is depicted in Figure 6. Each data point is the geometric mean of 15 trials, using one downlink antenna and the transmit array only, with one subarray. Zone 1 has a "flatter" angle more toward the receive array side of the BS, while zone 5 is more toward the transmit side, as shown in Figure 4.

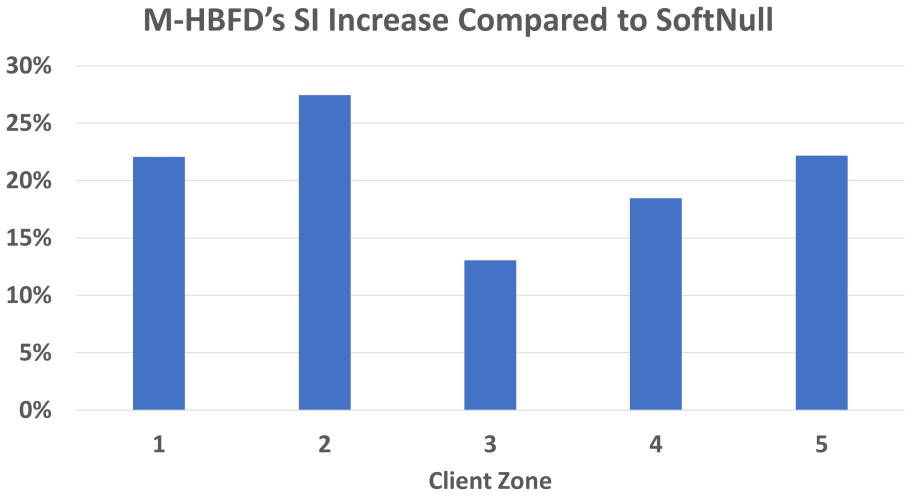

Figure 6. Effect of client zone on M-HBFD's SI compared to SoftNull. The total SI created at the BS by M-HBFD is 15–25% higher than the SI generated by SoftNull.

There is a larger difference in SI when communicating in zones 1 and 2. This indicates that M-HBFD shows weakness when beams are angled in the vicinity of the receive array. Further, the SI is also relatively high when clients are in the opposite direction, in zone 5. Finally, we observe that M-HBFD creates 15–25% higher SI at the BS compared to SoftNull.

7.3. Self-Interference

The effect of array size, number of clients, and number of effective antennas on SI compared to SoftNull is shown in Figure 7. Each data point is the geometric mean of 15 trials.

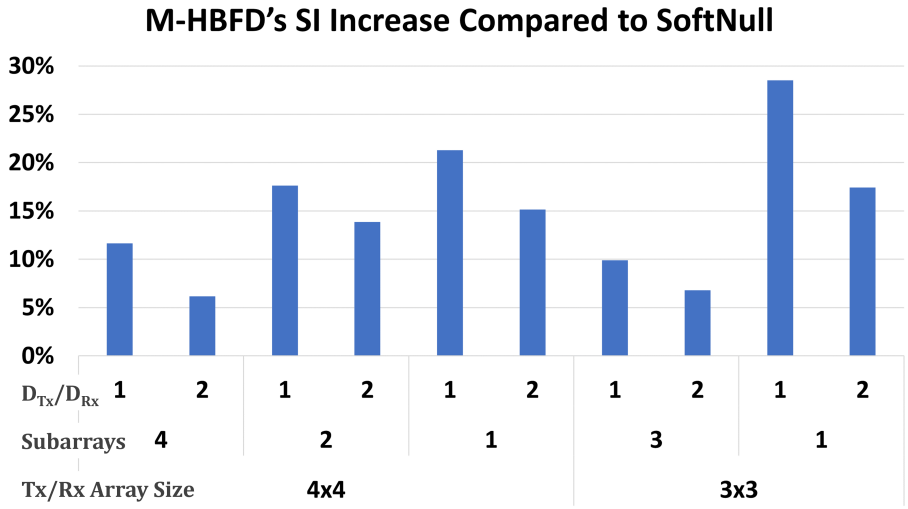

Figure 7. Effect of array size (bottom label, and denoted by Tx/Rx Array Size row), number of subarrays (middle label, and denoted by Subarrays row), and number of effective antennas per row (top label, and denoted by D_{Tx}/D_{Rx} row) on SI compared to SoftNull.

SI in M-HBFD was higher than SoftNull in all cases, with values ranging from 6–29% higher. The difference is smaller when using two effective antennas per row rather than one, or when communicating with more clients simultaneously.

Even the maximum performance advantage for SoftNull is only 29%, which means that a large amount of SI in our results is either easily canceled by both SoftNull and M-HBFD, or un-cancellable by either.

Adding more effective antennas reduces SoftNull's SI advantage. This indicates that M-HBFD is successfully canceling a certain amount of SI and additional effective antennas being repurposed from beamforming to SI cancellation would not be as useful. SoftNull, meanwhile, is more able to utilize the additional resources for additional SI cancellation, and so performs better relative to M-HBFD with two effective antennas per row.

Increasing the number of clients (increasing the number of subarrays in M-HBFD) decreases the difference in SI. This indicates MU-MIMO algorithms may reduce or eliminate the performance gap with fully digital algorithms as BSs get larger and communicate with more clients at once.

7.4. Capacity

The effect of array size, number of clients, and number of effective antennas on total sum capacity compared to SoftNull is shown in Figure 8. Each data point is the geometric mean of 15 trials. In all scenarios, the total capacity was within 15% of SoftNull.

In most array sizes and numbers of subarrays, using more effective antennas increased the relative performance of M-HBFD compared to SoftNull. These results are similar to the results for self-interference, but less pronounced. While we concluded above that SoftNull was better able to utilize additional cancellation resources, note that, when communicating with a single device per subarray, going from one effective antenna per row to two is

essentially doubling the directionality of the beamforming. Therefore, the disadvantage of M-HBFD is muted after accounting for increases in capacity from beamforming gain.

On average, using the larger 4×4 transmit and receive arrays had a slightly positive effect on the performance of M-HBFD compared to SoftNull.

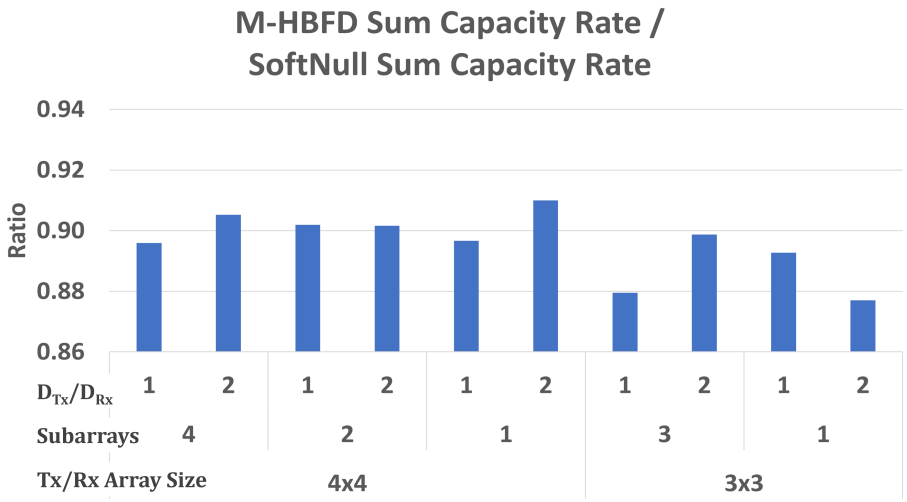

Figure 8. Effect of array size ((bottom), denoted by Tx/Rx Array Size row), number of subarrays ((middle), denoted by Subarrays row), and number of effective antennas per row ((top), denoted by D_{Tx}/D_{Rx} row) on capacity compared to SoftNull.

7.5. Capacity per RF Chain

The effect of array size, number of clients, and number of effective antennas on total sum capacity compared to SoftNull is shown in Figure 9. Each data point is the geometric mean of 15 trials. Note this is the same data as for our capacity comparison, but divided by the number of RF chains. In all cases, M-HBFD performs at least twice as well as SoftNull and, in the extreme case, achieves 14 times the capacity.

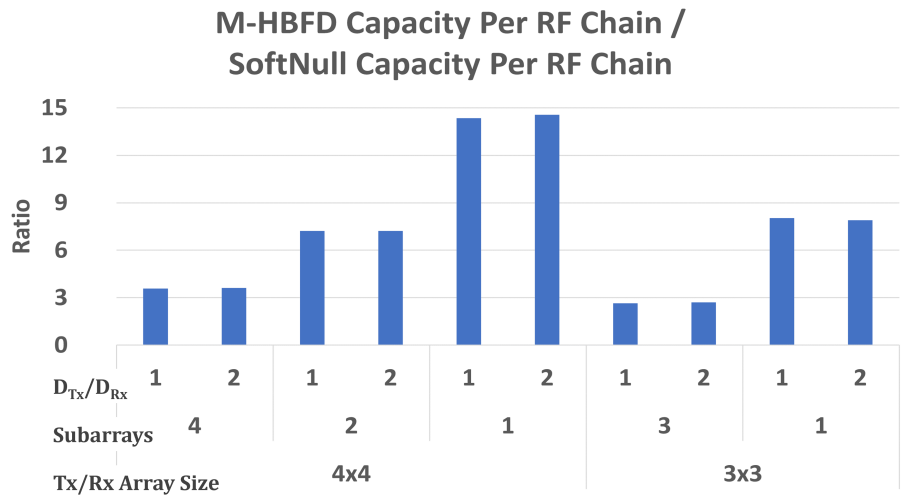

Figure 9. Effect of array size ((bottom), denoted by Tx/Rx Array Size row), number of subarrays ((middle), denoted by Subarrays row), and number of effective antennas per row ((top), denoted by D_{Tx}/D_{Rx} row) on capacity compared to SoftNull, normalized by number of RF chains used.

The advantage of our hybrid architecture MU-MIMO algorithm over fully digital algorithms is properly emphasized with these results. SoftNull, which uses a full RF chain for each antenna, is at a severe disadvantage to M-HBFD, which only uses a full RF chain for each subarray.

M-HBFD's performance gains diminish as the number of clients increases. However, this effect is due to dividing the stable total capacity over an increasing number of RF chains used. In the case of a 4×4 transmit and receive array with 4 subarrays each, M-HBFD still achieves 3 times the capacity per RF chain. If the number of clients increased to the point where the RF chains used by M-HBFD approached the number of antennas, we would expect the performance of both algorithms to degrade, and the relative advantage may end up reversing. However, using this many RF chains defeats the purpose of our assumed architecture in the first place.

M-HBFD scales better with array size. In the case of one subarray, where the whole transmit or receive array is used to communicate with one client each, going from an 18-antenna array to a 32-antenna array nearly doubles the number of RF chains used in SoftNull but has no effect on the number used in M-HBFD, leading to a capacity rate per RF chain for M-HBFD of almost two times.

8. Conclusions

In this paper, we conducted an experiment-based comparison between fully digital and hybrid beamforming radio architectures for many-antenna FD wireless systems. We designed a MU-MIMO hybrid architecture FD algorithm and implemented it and a leading digital architecture algorithm on programmable hardware and collected over-the-air channel data to compare the performance of the two systems in terms of SI cancellation and system capacity. We showed that the hybrid beamforming architecture achieves a comparable SI and capacity rate to the leading fully digital solution, despite requiring fewer RF chains, and decisively outperformed fully digital algorithms on a per-RF chain basis. For our future work, we plan to evaluate these techniques in even larger many-antenna BSs and apply similar experiments in low-scattering outdoor environments.

Author Contributions: Conceptualization, G.M., E.A., J.C., S.G. and S.M.H.; methodology, G.M. and E.A.; software, G.M.; validation, G.M.; formal analysis, G.M.; investigation, G.M.; resources, E.A.; data curation, G.M.; writing—original draft preparation, G.M.; writing—review and editing, G.M., E.A., J.C., S.G. and S.M.H.; visualization, G.M.; supervision, E.A.; project administration, E.A.; funding acquisition, E.A. and J.C. All authors have read and agreed to the published version of the manuscript.

Funding: This research was supported in part by an NSF grant (CNS 1910517).

Conflicts of Interest: The authors declare no conflict of interest.

Abbreviations

The following abbreviations are used in this manuscript:

BS	base station
FD	full-duplex
SI	self-interference
RF chain	radio frequency chain
MU-MIMO	multi-user multiple-input multiple-output
FPGA	field programmable gate array
PAFD	phased array full-duplex
LTS	long training sequence

References

1. Dey, I.; Salvo Rossi, P. Probability of outage due to self-interference in indoor wireless environments. *IEEE Commun. Lett.* **2017**, *21*, 8–11. [CrossRef]
2. Ghous, M.; Hassan, A.K.; Abbas, Z.H.; Abbas, G. Modeling and analysis of self-interference impaired two-user cooperative MIMO-NOMA system. *Phys. Commun.* **2021**, *48*, 101441. [CrossRef]
3. Choi, J.I.; Jain, M.; Srinivasan, K.; Levis, P.; Katti, S. Achieving single channel, full duplex wireless communication. In Proceedings of the Sixteenth Annual International Conference on Mobile Computing and Networking, Chicago, IL, USA, 20–24 September 2010; pp. 1–12.

4. Duarte, M.; Sabharwal, A. Full-duplex wireless communications using off-the-shelf radios: Feasibility and first results. In Proceedings of the 2010 Conference Record of the Forty Fourth Asilomar Conference on Signals, Systems and Computers, Pacific Grove, CA, USA, 4–7 November 2010; pp. 1558–1562.
5. Duarte, M.; Dick, C.; Sabharwal, A. Experiment-driven characterization of full-duplex wireless systems. *IEEE Trans. Wirel. Commun.* **2012**, *11*, 4296–4307. [CrossRef]
6. Jain, M.; Choi, J.I.; Kim, T.; Bharadia, D.; Seth, S.; Srinivasan, K.; Levis, P.; Katti, S.; Sinha, P. Practical, real-time, full duplex wireless. In Proceedings of the 17th Annual International Conference on Mobile Computing and Networking, Bologna, Italy, 11–13 October 2021; pp. 301–312.
7. Bharadia, D.; McMilin, E.; Katti, S. Full duplex radios. In Proceedings of the ACM SIGCOMM 2013 Conference on SIGCOMM, Hong Kong, China, 12–16 August 2013; pp. 375–386.
8. Aryafar, E.; Khojastepour, M.A.; Sundaresan, K.; Rangarajan, S.; Chiang, M. MIDU: Enabling MIMO full duplex. In Proceedings of the 18th Annual International Conference on Mobile Computing and Networking, Istanbul, Turkey, 22–26 August 2012; pp. 257–268.
9. Bliss, D.; Parker, P.; Margetts, A. Simultaneous transmission and reception for improved wireless network performance. In Proceedings of the 2007 IEEE/SP 14th Workshop on Statistical Signal Processing, Madison, WI, USA, 26–29 August 2007; pp. 478–482.
10. Duarte, M.; Sabharwal, A.; Aggarwal, V.; Jana, R.; Ramakrishnan, K.; Rice, C.W.; Shankaranarayanan, N. Design and characterization of a full-duplex multiantenna system for WiFi networks. *IEEE Trans. Veh. Technol.* **2013**, *63*, 1160–1177. [CrossRef]
11. Aryafar, E.; Keshavarz-Haddad, A. PAFD: Phased Array Full-Duplex. In Proceedings of the IEEE INFOCOM 2018—IEEE Conference on Computer Communications, Honolulu, HI, USA, 15–19 April 2018; pp. 261–269. [CrossRef]
12. Chen, T.; Dastjerdi, M.B.; Krishnaswamy, H.; Zussman, G. Wideband Full-Duplex Phased Array with Joint Transmit and Receive Beamforming: Optimization and Rate Gains. *IEEE ACM Trans. Netw.* **2021**, *29*, 1591–1604. [CrossRef]
13. Everett, E.; Shepard, C.; Zhong, L.; Sabharwal, A. SoftNull: Many-Antenna Full-Duplex Wireless via Digital Beamforming. *IEEE Trans. Wirel. Commun.* **2016**, *15*, 8077–8092. [CrossRef]
14. Payami, S.; Khalily, M.; Araghi, A.; Loh, T.H.; Cheadle, D.; Nikitopoulos, K.; Tafazolli, R. Developing the First mmWave Fully-Connected Hybrid Beamformer with a Large Antenna Array. *IEEE Access* **2020**, *8*, 141282–141291. [CrossRef]
15. Shepard, C.; Yu, H.; Anand, N.; Li, E.; Marzetta, T.; Yang, R.; Zhong, L. Argos: Practical Many-Antenna Base Stations. In Proceedings of the 18th Annual International Conference on Mobile Computing and Networking, Istanbul, Turkey, 22–26 August 2012; Association for Computing Machinery: New York, NY, USA, 2012. Mobicom'12. pp. 53–64. [CrossRef]
16. Yang, Q.; Li, X.; Yao, H.; Fang, J.; Tan, K.; Hu, W.; Zhang, J.; Zhang, Y. BigStation: Enabling Scalable Real-Time Signal Processingin Large Mu-Mimo Systems. *SIGCOMM Comput. Commun. Rev.* **2013**, *43*, 399–410. [CrossRef]
17. Xie, X.; Chai, E.; Zhang, X.; Sundaresan, K.; Khojastepour, A.; Rangarajan, S. Hekaton: Efficient and Practical Large-Scale MIMO. In Proceedings of the 21st Annual International Conference on Mobile Computing and Networking, New York, NY, USA, 3–5 November 2015; Association for Computing Machinery: New York, NY, USA, 2015. MobiCom'15. pp. 304–316. [CrossRef]
18. Gu, X.; Paidimarri, A.; Sadhu, B.; Baks, C.; Lukashov, S.; Yeck, M.; Kwark, Y.; Chen, T.; Zussman, G.; Seskar, I.; et al. Development of a Compact 28-GHz Software- Defined Phased Array for a City-Scale Wireless Research Testbed. In Proceedings of the 2021 IEEE MTT-S International Microwave Symposium (IMS), Atlanta, GA, USA, 6–11 June 2021; pp. 803–806. [CrossRef]
19. López-Valcarce, R.; Martínez-Cotelo, M. Full-Duplex mmWave Communication with Hybrid Precoding and Combining. In Proceedings of the 2020 28th European Signal Processing Conference (EUSIPCO), Amsterdam, The Netherlands, 8–21 January 2021; pp. 1752–1756. [CrossRef]
20. Wang, G.; Yang, Z.; Gong, T.; Xie, C. Self-Interference Cancellation Based Hybrid Beamforming Design for Full-Duplex mmWave Communication with Partially-Connected Structures. In Proceedings of the 2020 IEEE 20th International Conference on Communication Technology (ICCT), Nanning, China, 28–31 October 2020; pp. 366–371. [CrossRef]
21. López-Valcarce, R.; González-Prelcic, N. Analog beamforming for Full-Duplex Millimeter Wave Communication. In Proceedings of the 2019 16th International Symposium on Wireless Communication Systems (ISWCS), Oulu, Finland, 27–30 August 2019; pp. 687–691. [CrossRef]
22. Alexandropoulos, G.C.; Islam, M.A.; Smida, B. Full Duplex Hybrid A/D Beamforming with Reduced Complexity Multi-Tap Analog Cancellation. In Proceedings of the 2020 IEEE 21st International Workshop on Signal Processing Advances in Wireless Communications (SPAWC), Atlanta, GA, USA, 26–29 May 2020; pp. 1–5. [CrossRef]
23. Cao, Y.; Zhou, J. Integrated Self-Adaptive and Power-Scalable Wideband Interference Cancellation for Full-Duplex MIMO Wireless. *IEEE J. Solid-State Circuits* **2020**, *55*, 2984–2996. [CrossRef]
24. Ordoñez, L.G.; Ferrand, P.; Duarte, M.; Guillaud, M.; Yang, G. On Full-Duplex Radios with Modulo-ADCs. *IEEE Open J. Commun. Soc.* **2021**, *2*, 1279–1297. [CrossRef]
25. Cummings, I.T.; Doane, J.P.; Schulz, T.J.; Havens, T.C. Aperture-Level Simultaneous Transmit and Receive with Digital Phased Arrays. *IEEE Trans. Signal Process.* **2020**, *68*, 1243–1258. [CrossRef]
26. Gowda, N.M.; Sabharwal, A. JointNull: Combining Partial Analog Cancellation with Transmit Beamforming for Large-Antenna Full-Duplex Wireless Systems. *IEEE Trans. Wirel. Commun.* **2018**, *17*, 2094–2108. [CrossRef]
27. Kodak, U.; Rupakula, B.; Zihir, S.; Rebeiz, G.M. 60-GHz 64- and 256-Element Dual-Polarized Dual-Beam Wafer-Scale Phased-Array Transceivers with Reticle-to-Reticle Stitching. *IEEE Trans. Microw. Theory Tech.* **2020**, *68*, 2745–2767. [CrossRef]

28. Mondal, S.; Singh, R.; Hussein, A.I.; Paramesh, J. A 25–30 GHz Fully-Connected Hybrid Beamforming Receiver for MIMO Communication. *IEEE J. Solid-State Circuits* **2018**, *53*, 1275–1287. [CrossRef]
29. Megson, G.; Aryafar, E. Many-Antenna Full-Duplex with Fully Digital and Hybrid Beamforming Radios. In Proceedings of the 2021 IEEE-APS Topical Conference on Antennas and Propagation in Wireless Communications (APWC), Honolulu, HI, USA, 9–13 August 2021. [CrossRef]
30. Renew Project Documentation. Available online: https://docs.renew-wireless.org/ (accessed on 1 September 2021).